HHS Public Access

Author manuscript

J Pathol. Author manuscript; available in PMC 2018 November 18.

Published in final edited form as:

J Pathol. 2018 March ; 244(3): 271–282. doi:10.1002/path.5001.

C/ebpα controls osteoclast terminal differentiation, activation, function, and postnatal bone homeostasis through direct regulation of Nfatc1

Wei Chen[1,*], **Guochun Zhu**[1], **Jun Tang**[1], **Hou-De Zhou**[2], and **Yi-Ping Li**[1,*]

[1]Department of Pathology, University of Alabama at Birmingham School of Medicine, Birmingham , Alabama 35294-2182, United States of America

[2]Department of Metabolism & Endocrinology, National Clinical Research Center for Metabolic Diseases, The Second Xiangya Hospital, Central South University, ChangSha, Hunan, China.

Abstract

Osteoclast lineage commitment and differentiation have been studied extensively, although the mechanism by which transcription factor(s) control osteoclast terminal differentiation, activation and function remains unclear. CCAAT/enhancer-binding protein α (C/ebpα) has been reported to be a key regulator of osteoclast cell lineage commitment, yet C/ebpα's roles in osteoclast terminal differentiation, activation and function and bone homeostasis, under physiological or pathological conditions, have not been studied because newborn C/ebpα null mice die within several hours after birth. Furthermore, the function of *C/ebpα* in osteoclast terminal differentiation, activation and function are largely unknown. Herein, we generated and analyzed an osteoclast-specific *C/ebpα* conditional knockout (CKO) mouse model via *Ctsk-Cre* mice and found that C/ebpα-deficient mice exhibited a severe osteopetrosis phenotype due to impaired osteoclast terminal differentiation, activation and function, including mildly reduced osteoclast number, impaired osteoclast polarization, actin formation, and bone resorption, which demonstrated the novel function of C/ebpα in cell function and terminal differentiation. Interestingly, C/ebpα deficiency did not affect bone formation or monocyte/macrophage development. Our results further demonstrated that C/ebpα deficiency suppressed the expression of osteoclast functional genes, *e.g.* encoding Cathepsin K (*Ctsk*), Atp6i (*Tcirg1*) and osteoclast regulator genes, *e.g.* encoding c-fos (*Fos*), and nuclear factor of activated T-cells 1 (*Nfatc1*), while having no effect on Pu.1 (*Spi1*) expression. Promoter activity mapping and ChIP assay defined the critical cis-regulatory element (CCRE) in the promoter region of *Nfatc1*, and also showed that the CCREs were directly associated with C/ebpα, which enhanced the promoter's activity. The deficiency of C/ebpα in

[*]Correspondence to: **Yi-Ping Li**, Department of Pathology, University of Alabama at Birmingham, SHEL 810, 1825 University Blvd, Birmingham, AL 35294-2182, USA, Tel: 205-975-2606, Fax: 205-975-4919, yipingli@uabmc.edu and **Wei Chen**, Department of Pathology, University of Alabama at Birmingham, SHEL 815, 1825 University Blvd, Birmingham, AL 35294-2182, USA, Tel: 205-975-2605, Fax: 205-975-4919, weichen@uabmc.edu.

Author contributions statement

Study design: YPL, WC. Study conduct: WC, GZ, JT. Data collection and analysis: GZ, WC, JT and YPL. Drafting manuscript: YPL, WC, GZ, JT, and HDZ. Revising manuscript: YPL, WC, GZ, and HDZ. All authors approved the final version of the manuscript for submission. YPL (yipingli@uabmc.edu) and WC (weichen@uabmc.edu) take responsibility for the integrity of data analysis.

The authors declare no competing financial interests

osteoclasts completely blocked ovariectomy-induced bone loss, indicating C/ebpα is a promising new target for the treatment of osteolytic diseases.

Keywords

Cathepsin K; C/ebpα; Nfatc1; Osteoclast function; Terminal differentiation

Introduction

Osteoclasts (OCs) are multinucleated cells of the hematopoietic origin that play indispensable roles in skeletal development, bone remodeling and bone homeostasis. Excessive osteoclastic activity from defective osteoclastogenesis and impaired osteoclast function leads to many metabolic bone diseases (*e.g.* osteoporosis, arthritis, and periodontal diseases). Osteoclasts originate from monocytic precursors of the hematopoietic cell lineage upon stimulation with the macrophage-colony stimulation factor (M-CSF) and receptor activator of nuclear factor-κβ (RANK) ligand (RANKL) [1]. Despite the fact that some transcription factors which regulate osteoclast lineage commitment and differentiation have been characterized (the Finkel-Biskis-Jinkins osteosarcoma oncogene [c-fos*; Fos*], proviral integration 1 [Pu.1; *Spi1*], nuclear factor-kappaB [NF-κB; *Nfkb1*], and nuclear factor of activated T-cells 1 [Nfatc1; *Nfatc1*]), the mechanism underlying transcription factor regulation of osteoclast terminal differentiation, maturation, and function remains unclear [2].

CCAAT/enhancer binding protein α (C/ebpα) dimerizes via its leucine zipper (LZ) domain and binds to DNA via its basic region to activate transcription through its N-terminal trans-activation domains [3,4]. Early mutational events ultimately leading to acute myeloid leukemia (AML) often involve abrogation of C/ebpα expression and/or function [5]. The peripheral blood of mice lacking C/ebpα have significantly fewer granulocytes and monocytes [3], indicating C/ebpα plays important roles in monocyte lineage specification. We have recently identified C/ebpα as the CCRE binding protein at a proximal region of the promoter of *Ctsk,* encoding the osteoclast-specific Cathepsin K [6], and that C/ebpα is essential for osteoclast lineage commitment [6,7]. Although C/ebpα is a well-established lineage regulatory determinant in early hematopoietic development [5,8,9], several studies have also suggested it has multiple functions in several cell types [10–13], C/ebpα roles in postnatal skeletal development and bone homeostasis has not been studied since newborn C/ebpα null mice die within several hours after birth [4]. Additionally, the mechanisms underlying C/ebpα roles in postnatal physiological and pathological skeletal development remain elusive.

In this study, we generated a novel osteoclast-specific *C/ebpα* deletion mouse model to examine C/ebpα's roles in osteoclast activation and function, as well as to characterize the regulatory roles of C/ebpα in terminal differentiation stages of cells of the hematopoietic origin. We discovered that C/ebpα controls osteoclast terminal differentiation, activation, function, and postnatal bone homeostasis. Further, we found C/ebpα directly regulates *Nfatc1* expression and defined the CCREs in the promoter regions of *Nfatc1*, and that

conditional knockout of C/ebpα completely protected mice against ovariectomy-induced bone loss.

Materials and Methods

Generation of *C/ebpα$^{f/f}$Ctsk-Cre* mice.

C/ebpα$^{f/f}$ mice [9,14] were crossed with *Ctsk*-Cre knock-in mice. Male *C/ebpα*$^{F/+}$*Ctsk*-Cre and female *C/ebpα*$^{F/+}$*Ctsk*-Cre mice were crossed to obtain *C/ebpα$^{f/f}$Ctsk-Cre* and *C/ebpα$^{f/f}$* mice. The investigators were not blinded during allocation, animal handling, and endpoint measurements. Genotyping by PCR was carried out as described [15].

Histomorphometric analysis.

Samples were non-decalcified hard-tissue sections processed as described [16,17]. Analysis of sections was performed using the NIH program ImageJ as described [18].

Mouse bone marrow (MBM) and osteoclast-like cells.

MBM was obtained as described [19,20]. MBM was cultured in α-MEM (Invitrogen Carlsbad, CA, USA) with 10% FBS (Invitrogen) containing M-CSF (20ng/ml). After 1 day, cells were further cultured in the presence of 10 ng/ml soluble RANKL (Peprotech Rocky Hill, NJ, USA) and M-CSF (10 ng/ml R&D Systems, Minneapolis, MN, USA).

Cell staining for F-actin rings.

F-actin ring formation was evaluated as previously depicted [21]. Microscopy and 3-D construction were performed as described [22].

Acridine orange staining.

Acid production was determined using acridine orange as described previously [23]. The experiment was performed in duplicate on four independent occasions in a 12- or 6-well plate.

Promoter Analyses.

The mouse *Nfatc1* promoter was amplified using PCR from BAC clones provided by the BACPAC Resource Center at Children's Hospital Oakland Research Institute. Luciferase activity was measured as described [6,17].

Ovariectomy (OVX) Procedure.

C/ebpα$^{f/f/Δ}$ and *C/ebpα$^{f/f}$* mice were dorsal ovariectomized or sham-operated under anesthesia as described [24] . At three months post-operation, femurs and uteri were harvested for phenotypic and radiological analysis as previously described [25].

Statistical Analysis.

Experimental data are reported as mean±SEM or mean±SD of triplicate independent samples with both male and female mice in each group. Data were analyzed with Student's t-test or two-way ANOVA using GraphPad Prism statistical program. P values <0.05 were

considered significant. *p<0.05, **p<0.01, ***p<0.005. NS, not significant. Error bars depict SEM or SD as mentioned in individual figure legends

Results

C/ebpα$^{f/f}$*Ctsk-Cre* mice display an osteopetrotic phenotype that becomes accentuated as mice aged.

Newborn C/ebpα null mice die within several hours after birth so we were unable to use a conventional knockout to study C/ebpα's function in later stages of osteoclastogenesis and osteoclast activation and function *in vivo*. Therefore, we generated the CKO model, *C/ebpα*$^{f/f}$*Ctsk-Cre*, using osteoclast-specific *Ctsk-Cre* mediated targeted disruption of *C/ebpα* to further characterize C/ebpα's role in osteoclast homeostasis. Compared to wild type mice, heterozygous *Ctsk-Cre* and *C/ebpα*$^{f/f}$ had no detectable bone phenotype; *C/ebpα*$^{f/f}$ mice hence served as control group in this study (supplementary material, Figure S1B). During early stages of skeletal development (1 wk), male and female *C/ebpα*$^{f/f}$*Ctsk-Cre* mice exhibited an increase in bone radiodensity indicating osteopetrosis (Figure 1A). Bone radiographs were also examined at various time points in adult and aged mice (12 and 22 wk); the existing osteopetrotic condition became progressively worse in older *C/ebpα*-deficient mice compared to their WT littermates (Figure 1B,C). Further analysis and quantification of *C/ebpα*$^{f/f}$*Ctsk-Cre* and *C/ebpα*$^{f/f}$ mouse cortical bone showed no significant difference between the periosteum circumference of 12- and 22-wk old *C/ebpα*$^{f/f}$*Ctsk-Cre* and *C/ebpα*$^{f/f}$ mice, but a significant decrease in the endosteum circumference in the *C/ebpα*$^{f/f}$*Ctsk-Cre* mice compared to the *C/ebpα*$^{f/f}$ mice (supplementary material, Figure S1C). Analysis of mouse cranial development in 2, 4, 8, and 12-wk-old mice showed no overt effects of CKO on tooth eruption or skull phenotype (Figure 1D). When compared to that in *C/ebpα*$^{f/f}$ mice, the serum concentration of carboxy-terminal collagen crosslinks (CTX; bone resorption marker) decreased by nearly two-fold and surprisingly by almost four-fold in 12-wk-old and 22-wk-old *C/ebpα*$^{f/f}$*Ctsk-Cre* mice, respectively (Figure 1E). Micro-computed tomography (μ-CT) analysis of the distal femora of 12-wk-old female *C/ebpα*$^{f/f}$*Ctsk-Cre* mice revealed that femurs from mutant mice had increased trabecular numbers and higher ratios of bone volume/tissue volume compared to that of *C/ebpα*$^{f/f}$ mice (Figure 1F,H). Interestingly, while 12-wk-old *C/ebpα*$^{f/f}$*Ctsk-Cre* mice only showed a mild osteopetrotic phenotype (Figure 1F,H), older *C/ebpα*$^{f/f}$*Ctsk-Cre* mice (22-wk-old) experienced a much more severe osteopetrotic condition that was marked by a significant increase in bone density (Figure 1G,I). Our data suggested that Ctsk-Cre mediated CKO of *C/ebpα* results in osteopetrosis that was accentuated as mice aged.

Impaired osteoclast polarization and function contribute to the osteopetrotic phenotype displayed by *C/ebpα*$^{f/f}$*Ctsk-Cre* mice.

Through H&E staining, newborn *C/ebpα*$^{f/f}$*Ctsk-Cre* mice exhibited an enhanced bone trabecular volume compared to *C/ebpα*$^{f/f}$ control (Figure 2A). Furthermore, TRAP staining revealed that CKO of *C/ebpα*in osteoclasts significantly reduced the number of TRAP-positive multinucleated cells (MNCs) in newborn *C/ebpα*$^{f/f}$*Ctsk-Cre* mouse femurs (Figure 2B-**C**) suggesting defects in osteoclast terminal differentiation *in vivo*. Interestingly, examination of calcein-labeled mouse femurs using the mineral apposition rate (MAR) to

detect the differences in bone formation showed no significant changes in bone formation between mutant and WT femurs (Figure 2D,E), confirming that the reduced bone density was not caused by decreased bone formation. Consistently, H&E staining and Goldner's Trichrome staining indicated a significant increase in mineralized tissue in 22-wk-old *C/ebpα$^{f/f}$Ctsk-Cre* mice (Figure 2F,G). Higher magnification images showed that mutant mice lacked the gaps between the osteoclasts and trabecular bones (i.e. Howship's lacunae), due to reduced osteoclastic bone resorption (Figure 2G). Histomorphometric measurements based on Trichrome staining also confirmed that the severity of osteopetrosis persisted and increased over the course of bone development without affecting osteoblast number in *C/ebpα$^{f/f}$Ctsk-Cre* mice at 22 wk of age (Figure 2H). Since osteoclasts differentiate from cells of the hematopoietic origin, we sought to assess the status of monocyte/macrophage development in *C/ebpα$^{f/f}$Ctsk-Cre*. Flow cytometry was performed using 8-wk-old mouse bone marrow (MBM) to examine infiltration of CD11b+F4/80+ macrophages (Figure 2I) and CD11b+CD115+ osteoclasts (Figure 2J) in *C/ebpα$^{f/f}$Ctsk-Cre* mice. Although the number of macrophages in mutant mice remained similar to that of WT, the number of osteoclasts in CKO mice was significantly reduced (Figure 2K). Consistently, P1NP serum level (bone formation marker) remained unaltered between *C/ebpα$^{f/f}$Ctsk-Cre* and *C/ebpα$^{f/f}$*, indicating that bone formation rate in both long and flat bones were not affected by C/ebpα CKO (Figure 2L). These results show that osteoclast lineage-specific C/ebpα deletion impairs osteoclast terminal differentiation which results in reduced osteoclastic bone resorption leading to higher bone density *in vivo*.

C/ebpα deficiency impairs activation and function of multinucleated osteoclasts *in vitro*.

In order to determine whether *C/ebpα* excision has an effect on mature osteoclast function and structure, MBM from 6-wk-old *C/ebpα$^{f/f}$Ctsk-Cre* and WT mice was stimulated by M-CSF (10 ng/mL) and RANKL (10 ng/mL) to promote the formation of mature MNCs (defined as TRAP-positive cells with three or more visible nuclei). We then performed extensive *in vitro* osteoclast differentiation and functional assays using RANKL/M-CSF induced *C/ebpα$^{f/f}$Ctsk-Cre* MBM at the end of a 5 d osteoclastogenic culture. Although reduced TRAP activity was evident in CKO, MNC formation was still possible in *C/ebpα*-deficient mice (Figure 3A,D), further confirming a mild defect in osteoclast formation. In osteoclast functional assay, we found that extracellular acidification was almost absent (Figure 3B,E) and that actin formation was defective (Figure 3C) in *C/ebpα$^{f/f}$Ctsk-Cre* compared to the *C/ebpα$^{f/f}$* control. We then seeded the same number of induced MBM cells on each bone slice. Here, TRAP activity and actin ring formation was disrupted or almost absent in *C/ebpα*-deficient MBM indicating their inactive status (Figure 3F,G). We further examined the molecular distribution of Ctsk by performing immunofluorescence staining of the induced osteoclast cells on bone slices. Ctsk expression in mature, multinucleated osteoclasts obtained from WT culture was indeed colocalized with osteoclast ruffled borders, *Ctsk* expression in osteoclasts depleted of *C/ebpα* showed an approximate seven-fold reduction (Figure 3H) and actin ring formation on bone slice of the *C/ebpα*-deficient OCs was inhibited (Figure 3I). Thus, it is possible that *C/ebpα* plays a critical role in regulating *Ctsk* expression, thereby resulting in its critical role in osteoclast function. Furthermore, wheat germ agglutinin (WGA) staining and scanning electron microscopy (SEM) analysis conclusively confirmed defective osteoclastic bone resorption resulting from

targeted disruption of *C/ebpα* (Figure 3J,K), in which bone resorption pits were significantly reduced compared to *C/ebpα*$^{f/f}$ control (Figure 3L). Collectively, these data indicate that *C/ebpα* CKO impairs cell activation and function in osteoclast terminal differentiation, and that *C/ebpα* is essential for *in vitro* bone resorption of osteoclasts.

Ctsk-Cre mediated targeted disruption of *C/ebpα* significantly reduces the expression of osteoclast regulator and functional genes in osteoclasts.

To further examine *C/ebpα*'s role in osteoclast activation and function as well as gene expression in situ, Immunofluorescence (IF) analysis was carried out to examine gene expression using newborn mouse serial paraffin sections (Figure 4). When compared to the negative control (Figure 4A), C/ebpα was identified in osteoclasts and mononuclear pre-osteoclasts or Acp5^{+} cells (Figure 4B yellow merged area indicates overlap). For the quantification of IF signals, we used NIH image software (ImageJ) to perform counts; the percentage of positive cells is the number of positive cells expressing the IF-detected protein divided by the number of TRAP-positive cells where we counted only the cells that express both Acp5 (bone resorption marker) and the protein of interest as shown in the merged images. C/ebpα was efficiently ablated in *C/ebpα*$^{f/f}$*Ctsk-Cre* osteoclasts (Figure 4B, lower panel merged image). Mutant mice had a nearly two-fold reduction in numbers of Acp5-positive cells and a four-fold reduction in numbers of C/ebpα-positive cells (Figure 4B,G). Ctsk-positive cells were also reduced by more than four-fold in *C/ebpα*$^{f/f}$*Ctsk-Cre* osteoclasts compared to the *C/ebpα*$^{f/f}$ mice (Figure 4C,G). We also found substantially lower c-fos expression in *C/ebpα*-deficient mice (Figure 4D,G). Interestingly, Pu.1 expression levels remained almost identical between *C/ebpα*$^{f/f}$*Ctsk-Cre* and *Ctsk-Cre* mice (Figure 4E,G). Importantly, Nfatc1 expression decreased by more than three-fold in mutant mice compared to *C/ebpα*$^{f/f}$ mice (Figure 4F,G). Paraffin serial sections from newborn and post-natal day 1 *C/ebpα*$^{f/f}$*Ctsk-Cre* and the control *Ctsk*-Cre mouse femurs were also subjected to immunohistochemical (IHC) and H&E staining respectively (supplementary material, Figure S2). Magnified images of H&E staining of the bone collar region of post-natal day 1 *C/ebpα*$^{f/f}$*Ctsk-Cre* mice femurs showed no significant changes in osteoblast numbers compared to the *Ctsk*-Cre control (supplementary material, Figure S2A). Compared to the *C/ebpα*$^{f/f}$ control, no changes in monocyte development [CD11b+ cells (monocyte marker)] were detected in *C/ebpα*$^{f/f}$*Ctsk-Cre* newborn mice (supplementary material, Figure S2B,C). c-fos, and Nfatc1 expression were evidently suppressed; however, Pu.1 remained almost unchanged compared to the control samples (supplementary material, Figure S2 D-F). We also found that no significant changes in the numbers of F4/80-positive macrophages between WT and mice lacking *C/ebpα* (supplementary material, Figure S2G,H). Taken together, our results demonstrated that *Ctsk-Cre*-mediated CKO of *C/ebpα* caused C/ebpα deficiency that inhibited the expression of osteoclast function and regulator genes at the protein level, and that C/ebpα deficiency no longer affects Pu.1 expression during later stages of osteoclast development.

C/ebpα CKO in *C/ebpα*$^{f/f}$*Ctsk-Cre* does not affect apoptosis in osteoclasts during early stages of cytokine and serum deprivation.

To determine the role of *C/ebpα* in apoptotic morphology in osteoclasts, apoptosis was induced by cytokine and serum deprivation for 6 h and detected by Hoechst 33258 staining

followed by staining of F-actin podosomal belts with rhodamine phalloidin of the induced osteoclasts. Although the positive control exhibited apoptosis with typical fragmentation, aggregation, and condensation (white arrows) of nuclei (supplementary material, Figure S3A), the apoptotic parameters were mostly similar in the WT and mutant cells (supplementary material, Figure S3B,C). Extensive apoptosis culture also showed that *C/ebpα*-deficient mature osteoclasts did not survive longer than WT cells during the first 12 h of the apoptotic test, whereas more *C/ebpα*$^{f/f}$*Ctsk-Cre* osteoclasts underwent apoptosis at 24 h (supplementary material, Figure S3D).

C/ebpα positively regulates the expression of osteoclast transcriptional regulators and osteoclast function genes.

To investigate the molecular mechanism underlying the role of *C/ebpα* in bone homeostasis, we examined the expression of the aforementioned osteoclast functional genes along with important osteoclast regulator genes in *C/ebpα*$^{f/f}$*Ctsk-Cre* (Figure 5A,B). Deletion of C/ebpα was confirmed by Western blot and qPCR analysis (Figure 5A,B). Quantitative protein analysis showed that deficiency of C/ebpα significantly reduced the expression of key osteoclast transcriptional factors (*e.g.* c-fos, Nfatc1) as well as important osteoclast function effectors (*e.g.* Ctsk, ATP6i) in CKO mice compared to the controls (i.e. *C/ebpα*$^{f/f}$ and *Ctsk-Cre*) (Figure 5A and supplementary material, Figure S4). Notably, Pu.1 expression remained unaltered in *C/ebpα*$^{f/f}$*Ctsk-Cre* mice compared to that of control groups (Figure 5A and supplementary material, Figure S4). At the transcript level, RT-qPCR analysis displayed a similar pattern in which deficiency of *C/ebpα* downregulated the levels of *Ctsk*, *ATP6i*, *c-fos*, *Nfatc1* and other critical osteoclast-specific genes, yet *Pu.1* levels remained unchanged (Figure 5B). Together, our results indicate that *C/ebpα* is a crucial regulator of osteoclast terminal differentiation, activation, and function through positively regulating osteoclast transcription regulators and osteoclast function genes.

C/ebpα directly upregulates *Nfatc1* expression by associating with its promoters.

Since we have previously identified potential binding sites for C/ebpα in the *c-fos* promoter, we used a ChIP assay to further determine the binding patterns between C/ebpα and the *Nfatc1* (−2990/+10) promoter regions using DNA prepared from MBM induced by RANKL and M-CSF for 4 d as described [26,27]. ChIP analysis was performed using an anti-C/ebpα antibody. DNA was pulled down, amplified, and analyzed using primers shown in Figure 5C. ChIP input value using each primer represents the binding efficiency of an adjacent region around the location of the primer pair. We found several C/ebpα binding sites in the *Nfatc1* promoter region (−2990/+10), and we also found that *Nfatc1* primer pair 2 (−1832/−1771) and primer pair 3 (−1353/−1237) in the *Nfatc1* promoter region (−2990/+10) resulted in significantly high ChIP input values, indicating that C/ebpα binding sites at −1852, −1740, −1375 and −1281 in *Nfatc1* promoter region are most efficient (Figure 5D). Macrophage-like RAW264.7 cells were induced by RANKL and M-CSF for 2 days to promote the formation of multinucleated osteoclasts, and then transfected with the corresponding luciferase reporter vectors. Luciferase assay showed the highest activity in the longest *Nfatc1* promoter fragment (−2768/+10) and gradually decreased in shorter fragments; however (−1345/+10) promoter fragment still retained significantly higher luciferase activity compared to the pGL3-basic vector control (Figure 5E). Thus, C/ebpα is

able to directly bind to the *Nfatc1* promoter to regulate gene expression, and the binding sites −1852, −1740, −1374, and −1281 are critical in this interaction.

C/ebpα$^{f/f}$*Ctsk-Cre* mice exhibit protection against ovariectomy-induced bone loss.

In order to examine how C/ebpα regulates bone remodeling, we performed sham surgery or ovariectomy (OVX) on *C/ebpα*$^{f/f}$ and *C/ebpα*$^{f/f}$*Ctsk-Cre* mice. OVX in mice mimics estrogen-depletion-induced bone loss in postmenopausal women, and might provide a better support for the role of C/ebpα on pathologic bone loss. At 12 wk following the operations, mouse body size (Figure 6A) was first examined to confirm an effect of OVX in *C/ebpα*$^{f/f}$*Ctsk-Cre* and *C/ebpα*$^{f/f}$ mice. Radiographic images revealed that OVX-*C/ebpα*$^{f/f}$*Ctsk-Cre* femurs were protected against OVX-induced bone loss compared to control femurs (Figure 6B), even though uteri in post-OVX *C/ebpα*$^{f/f}$ and *C/ebpα*$^{f/f}$*Ctsk-Cre* were dramatically smaller in size compared to those in post-sham *C/ebpα*$^{f/f}$ mice (Figure 6C). Similarly, OVX-*C/ebpα*$^{f/f}$*Ctsk-Cre* mice were protected against bone loss when compared with sham-operated *C/ebpα*$^{f/f}$*Ctsk-Cre* and OVX-*Ctsk-Cre* controls (Figure 6D-F). When compared to sham *C/ebpα*$^{f/f}$, there was a significant bone density decrease in post-OVX *C/ebpα*$^{f/f}$ mice due to OVX induced estrogen-depletion (Figure 6G). At 12 wk post operation, femurs from OVX *C/ebpα*$^{f/f}$*Ctsk-Cre* mice retained significantly higher ratios of bone volume/tissue volume and increased trabecular numbers compared to sham- or OVX-*C/ebpα*$^{f/f}$ mice (Figure 6H). At the same time, no significant changes were found between sham- and OVX-*C/ebpα*$^{f/f}$*Ctsk-Cre* (Figure 6I). These findings suggest that C/ebpα deficiency in *C/ebpα*$^{f/f}$*Ctsk-Cre* mice protected mice from OVX-induced bone loss, which provides significant insights into the roles of *C/ebpα* in regulating bone density in normal and OVX conditions. *C/ebpα* may be a promising novel approach for the treatment of osteolytic diseases.

C/ebpα deficiency does not affect mouse body weight.

To further determine whether *C/ebpα* CKO caused runt phenotype in mutant mice, we examined the mouse body weights of *C/ebpα*$^{f/f}$ and *C/ebpα*$^{f/f}$*Ctsk-Cre* mice (Figure 6I,J). In the pathologically induced model, there was no change in mouse body weight across OVX and sham groups of mutant and wild-type mice (Figure 6J). In the physiological aging process, both male and female *C/ebpα*$^{f/f}$ and *C/ebpα*$^{f/f}$*Ctsk-Cre* mice exhibited similar size and body weight at various stages of skeletal development (Figure 6K, and supplementary material, Figure S6**A**).

Forced expression of C/ebpα in the absence of RANKL promotes osteoclastogenesis and upregulates the expression osteoclast-specific genes.

We used a retrovirus to express C/ebpα ectopically in MBM cells with only M-CSF (20ng/mL) stimulation. The retrovirus vector, pBMN-*C/ebpα*, was engineered to express *C/ebpα* and also GFP in order to measure transduction efficiency. MBM cells were transduced with pBMN-*C/ebpα* or with a control virus (pBMN-GFP) as described [28]. *C/ebpα* expression in MBM transfected with pBMN-*C/ebpα* became significantly higher than that in the control vector at 48 hr and continuously increased throughout the remaining time points (supplementary material, Figure S5A-B). At 96 h after M-CSF induction, GFP-positive cells

were visualized to measure transduction efficacy (supplementary material, Figure S5C). We also found that bone marrow with C/ebpα overexpression developed a significant higher number of TRAP+ cells (supplementary material, Figure S5D). The sensitivity of C/ebpα-overexpressing bone marrow in the absence of RANKL establishes the importance of C/ebpα in promoting $TRAP^+$ cells. RT-qPCR revealed a significant increases in *c-fos*, *Nfatc1*, *Ctsk*, and *Mmp9*, levels while *Pu.1* levels remained unchanged in pBMN-GFP-transfected MBM compared to wild-type and control vector (supplementary material, Figure S5E). TRAP activity was significantly enhanced in C/ebpα-overexpressing MBM cells seeded on bone slices compared to pBMN-GFP controls, indicating their activated bone resorption capability (supplementary material, Figure S5F). RANKL-independent osteoclast formation can be driven by IL-6 and TNF. Interestingly, C/ebpα overexpression significantly upregulated the expression of *Il6*, but not *Tnf*, pinpointing a possible mechanism underlying the RANKL-independent C/ebpα-mediated regulation of osteoclast homeostasis (supplementary material, Figure S5E). In addition, we examined the expression of *Ctsk* across various tissue types in 8-week-old wild-type mice, and found high levels of *Ctsk* not only in mature osteoclasts, but also in dendritic cells (supplementary material, Figure S6). Taken together, these results indicate a critical stimulatory role of C/ebpα in osteoclast terminal differentiation, activation and function.

Discussion

C/ebpα is an important transcriptional regulator of hematopoiesis, which acts through its ability to bind DNA and influence transcriptional activities of different genes. Recent studies have exclusively argued for the importance of *C/ebpα* in monocyte/macrophage and OC lineage allocation [8,29]. In this study, we found that *in vivo* osteoclast terminal differentiation in C/ebpα CKO mice was affected along with severely impaired osteoclastic bone resorption, which suggests that C/ebpα might play a critical yet independent role in osteoclast terminal differentiation. C/ebpα can be removed from the cell through an ubiquitin-proteasome system-mediated mechanism [30], hence RANKL may protect C/ebpα from being degraded, thereby leading to its high expression in the cytoplasm during osteoclastogenic induction. C/ebpα up-regulates *Nfatc1* expression through directly binding to a CCRE in the promoter region of *Nfatc1*, which then directly binds to osteoclast gene promoters to drive their expression. C/ebpα's effects on osteoclast terminal differentiation may also be enhanced by the direct interaction between C/ebpα and *C/ebpα* binding sites as a CCRE in the *Ctsk* (−47bp) promoter region [6]. Although studies to date have indicated that the lysosomal cysteine Ctsk is predominantly expressed in osteoclasts, we also found high level of *Ctsk* mRNA in dendritic cells (Figure S6). Notably, we recently discovered an important osteoimmune role that Ctsk plays in regulating the cytokine secretion in LPS and CpG-stimulated dendritic cells [31]. Hence, it is possible that beside its direct activity in inducing expression of important osteoclast regulator and function genes in osteoclasts, C/ebpα may indirectly affect osteoclast function through altering Ctsk expression in other tissues, specifically in dendritic cells, thereby mediating secretions of pro-inflammatory cytokines to activate RANKL-independent bone formation. Although our research previously showed that constitutive C/ebpα ablation significantly reduced *Pu.1* expression and that C/ebpα could play major roles in osteoclast lineage commitment [6], *Pu.1*

expression in *C/ebpα*$^{f/f}$*Ctsk-Cre* remained unchanged (Figs 4 and 5); indicating that C/ebpα no longer regulates *Pu.1* expression in pre-osteoclast and osteoclast stages as cell lineage determination has already taken place. It had been shown that some differentiation status-related epigenetic changes associated with *Pu.1* promoter region have the potential to repress *Pu.1* transcriptional activity. In contrast, *c-fos* (a key regulator of osteoclast-macrophage lineage determination) is significantly downregulated in *C/ebpα*$^{f/f}$*Ctsk-Cre* suggesting an important role for *c-fos* throughout osteoclast development, possibly due to direct interactions with the C/ebpα binding sites in the promoter region of the *c-fos* gene [6]. C/ebpα may also directly up-regulate osteoclast function genes (e.g. *Ctsk* and *Atp6i*) leading to the increase in expression of key osteoclast function genes, which can mediate osteoclastic bone resorption involving actin ring formation, extracellular acidification and matrix protein degradation.

C/ebpα deficiency in osteoclasts completely protected mice against OVX-induced bone loss, thus C/ebpα inhibitors may lead to desirable therapeutics and further optimize the current treatment options for local bone loss in periodontal disease. However, screening for effective C/ebpα inhibitors can be problematic in systemic osteolytic disorders, since C/ebpα is ubiquitously expressed and involved in proliferation arrest and the differentiation of multiple cell types. To overcome these limitations and further our current understanding of osteoclast biology, it is important to explore the mechanisms underlying how C/ebpα specifically regulates osteoclast activation and function, and to reveal effective upstream *C/ebpα* regulators that are specific to osteoclasts. Given its differential roles in different stages of cell development, understanding how C/ebpα regulates osteoclast terminal differentiation, activation and function also provides important mechanistic insights into osteoclast biology knowledge that can greatly benefit future research in the investigation of potential *C/ebpα* regulators, significant pathways in the pathogenesis of acute myeloid leukemia, as well as pointing to a new target for the development of future novel and effective treatments for osteolytic diseases.

Supplementary Material

Refer to Web version on PubMed Central for supplementary material.

Acknowledgements

We thank Ms. Diep Nguyen and Ms. Christie Paulson for their assistance with the manuscript; and Matthew McConnell for his bioinformatics analysis assistance. We thank Dr. Shigeaki Kato for the Cathepsin K-Cre mouse line gift. We appreciate the assistance of the Center for Metabolic Bone Disease at the University of Alabama at Birmingham (UAB) (P30 AR046031). We are also grateful for the assistance of the Small Animal Phenotyping Core, Metabolism Core, and Neuroscience Molecular Detection Core Laboratory at UAB (P30 NS0474666). This work was supported by National Institutes of Health [AR-44741 and DE-023813 to Y.P.L. and AR-070135 to W.C.].

References

1. Boyle WJ, Simonet WS, Lacey DL. Osteoclast differentiation and activation. Nature 2003; 423: 337–342. [PubMed: 12748652]
2. Soltanoff CS, Yang S, Chen W, et al. Signaling networks that control the lineage commitment and differentiation of bone cells. Crit Rev Eukaryotic Gene Express 2009; 19: 1–46.

3. Friedman AD. C/EBPalpha in normal and malignant myelopoiesis. Int J Hematol 2015; 101: 330–341. [PubMed: 25753223]
4. Ohlsson E, Schuster MB, Hasemann M, et al. The multifaceted functions of C/EBPalpha in normal and malignant haematopoiesis. Leukemia 2016; 30: 767–775. [PubMed: 26601784]
5. Schuster MB, Porse BT. C/EBPalpha in leukemogenesis: identity and origin of the leukemia-initiating cell. BioFactors (Oxford, England) 2009; 35: 227–231.
6. Chen W, Zhu G, Hao L, et al. C/EBPalpha regulates osteoclast lineage commitment. Proc Natl Acad Sci U S A 2013; 110: 7294–7299. [PubMed: 23580622]
7. Jules J, Chen W, Feng X, et al. CCAAT/Enhancer-binding Protein alpha (C/EBPalpha) Is Important for Osteoclast Differentiation and Activity. J Biol Chem 2016; 291: 16390–16403. [PubMed: 27129246]
8. Feng R, Desbordes SC, Xie H, et al. PU.1 and C/EBPalpha/beta convert fibroblasts into macrophage-like cells. Proc Natl Acad Sci U S A 2008; 105: 6057–6062. [PubMed: 18424555]
9. Welner RS, Bararia D, Amabile G, et al. C/EBPalpha is required for development of dendritic cell progenitors. Blood 2013; 121: 4073–4081. [PubMed: 23547051]
10. Bueno C, Sardina JL, Di Stefano B, et al. Reprogramming human B cells into induced pluripotent stem cells and its enhancement by C/EBPalpha. Leukemia 2016; 30: 674–682. [PubMed: 26500142]
11. Di Stefano B, Collombet S, Jakobsen JS, et al. C/EBPalpha creates elite cells for iPSC reprogramming by upregulating Klf4 and increasing the levels of Lsd1 and Brd4. Nat Cell Biol 2016; 18: 371–381. [PubMed: 26974661]
12. Friedman AD. C/EBPalpha induces PU.1 and interacts with AP-1 and NF-kappaB to regulate myeloid development. Blood Cells Mol Dis 2007; 39: 340–343. [PubMed: 17669672]
13. Kasakura K, Takahashi K, Itoh T, et al. C/EBPα controls mast cell function. FEBS Letters 2014; 588: 4645–4653. [PubMed: 25447519]
14. Zhang DE, Zhang P, Wang ND, et al. Absence of granulocyte colony-stimulating factor signaling and neutrophil development in CCAAT enhancer binding protein alpha-deficient mice. Proc Natl Acad Sci U S A 1997; 94: 569–574. [PubMed: 9012825]
15. Growney JD, Shigematsu H, Li Z, et al. Loss of Runx1 perturbs adult hematopoiesis and is associated with a myeloproliferative phenotype. Blood 2005; 106: 494–504. [PubMed: 15784726]
16. Yang S, Li YP. RGS10-null mutation impairs osteoclast differentiation resulting from the loss of [Ca2+]i oscillation regulation. Genes Dev 2007; 21: 1803–1816. [PubMed: 17626792]
17. Chen W, Yang S, Abe Y, et al. Novel pycnodysostosis mouse model uncovers cathepsin K function as a potential regulator of osteoclast apoptosis and senescence. Hum Mol Genet 2007; 16: 410–423. [PubMed: 17210673]
18. Jiang H, Chen W, Zhu G, et al. RNAi-Mediated Silencing of Atp6i and Atp6i Haploinsufficiency Prevents Both Bone Loss and Inflammation in a Mouse Model of Periodontal Disease. PloS one 2013; 8: e58599. [PubMed: 23577057]
19. Kelly KA, Tanaka S, Baron R, et al. Murine bone marrow stromally derived BMS2 adipocytes support differentiation and function of osteoclast-like cells in vitro. Endocrinology 1998; 139: 2092–2101. [PubMed: 9528998]
20. Kurland JI, Kincade PW, Moore MA. Regulation of B-lymphocyte clonal proliferation by stimulatory and inhibitory macrophage-derived factors. J Exp Med 1977; 146: 1420–1435. [PubMed: 303681]
21. Feng S, Deng L, Chen W, et al. Atp6v1c1 is an essential component of the osteoclast proton pump and in F-actin ring formation in osteoclasts. Biochem J 2009; 417: 195–203. [PubMed: 18657050]
22. Yang DQ, Feng S, Chen W, et al. V-ATPase subunit ATP6AP1 (Ac45) regulates osteoclast differentiation, extracellular acidification, lysosomal trafficking, and protease exocytosis in osteoclast-mediated bone resorption. J Bone Mineral Res 2012; 27: 1695–1707.
23. Li YP, Chen W, Liang Y, et al. Atp6i-deficient mice exhibit severe osteopetrosis due to loss of osteoclast-mediated extracellular acidification. Nature Genet 1999; 23: 447–451. [PubMed: 10581033]

24. Zhang Y, Wang L, Song Y, et al. Renin inhibitor aliskiren exerts beneficial effect on trabecular bone by regulating skeletal renin-angiotensin system and kallikrein-kinin system in ovariectomized mice. Osteoporos Int 2016; 27: 1083–1092. [PubMed: 26439241]

25. Wu M, Chen W, Lu Y, et al. Galpha13 negatively controls osteoclastogenesis through inhibition of the Akt-GSK3beta-NFATc1 signalling pathway. Nat Commun 2017; 8: 13700. [PubMed: 28102206]

26. Chen W, Ma J, Zhu G, et al. Cbfbeta deletion in mice recapitulates cleidocranial dysplasia and reveals multiple functions of Cbfbeta required for skeletal development. Proc Natl Acad Sci U S A 2014; 111: 8482–8487. [PubMed: 24850862]

27. Kuras L, Struhl K. Binding of TBP to promoters in vivo is stimulated by activators and requires Pol II holoenzyme. Nature 1999; 399: 609–613. [PubMed: 10376605]

28. Takayanagi H, Kim S, Koga T, et al. Induction and activation of the transcription factor NFATc1 (NFAT2) integrate RANKL signaling in terminal differentiation of osteoclasts. Dev Cell 2002; 3: 889–901. [PubMed: 12479813]

29. Xie H, Ye M, Feng R, et al. Stepwise reprogramming of B cells into macrophages. Cell 2004; 117: 663–676. [PubMed: 15163413]

30. Wang GL, Shi X, Haefliger S, et al. Elimination of C/EBPalpha through the ubiquitin-proteasome system promotes the development of liver cancer in mice. J Clin Invest 2010; 120: 2549–2562. [PubMed: 20516642]

31. Hao L, Zhu G, Lu Y, et al. Deficiency of cathepsin K prevents inflammation and bone erosion in rheumatoid arthritis and periodontitis and reveals its shared osteoimmune role. FEBS Letters 2015; 589: 1331–1339. [PubMed: 25896020]

*32. Nakamura T, Imai Y, Matsumoto T, et al. Estrogen prevents bone loss via estrogen receptor alpha and induction of Fas ligand in osteoclasts. Cell 2007; 130: 811–823. [PubMed: 17803905]

*33. Yang S, Hao L, McConnell M, et al. Inhibition of Rgs10 Expression Prevents Immune Cell Infiltration in Bacteria-induced Inflammatory Lesions and Osteoclast-mediated Bone Destruction. Bone Res 2013; 1: 267–281. [PubMed: 24761229]

*34. Su X, Floyd DH, Hughes A, et al. The ADP receptor P2RY12 regulates osteoclast function and pathologic bone remodeling. J Clin Invest 2012; 122: 3579–3592. [PubMed: 22996695]

*35. Gao B, Chen W, Hao L, et al. Inhibiting periapical lesions through AAV-RNAi silencing of cathepsin K. J Dent Res 2013; 92: 180–186. [PubMed: 23166044]

*36. Ma J, Chen W, Zhang L, et al. RNAi mediated silencing of Atp6i prevents both periapical bone erosion and inflammation in the mouse model of endodontic disease. Infect Immun 2012.

*37. Zhao H, Ito Y, Chappel J, et al. Synaptotagmin VII regulates bone remodeling by modulating osteoclast and osteoblast secretion. Dev Cell 2008; 14: 914–925. [PubMed: 18539119]

*38. Chen W, Li YP. Generation of mouse osteoclastogenic cell lines immortalized with SV40 large T antigen. J Bone Miner Res 1998; 13: 1112–1123. [PubMed: 9661075]

*39. Allaire JM, Darsigny M, Marcoux SS, et al. Loss of Smad5 leads to the disassembly of the apical junctional complex and increased susceptibility to experimental colitis. Am J Physiol Gastrointest Liver Physiol 2011; 300: G586–597. [PubMed: 21212325]

*40. Nijenhuis T, van der Eerden BC, Hoenderop JG, et al. Bone resorption inhibitor alendronate normalizes the reduced bone thickness of TRPV5(−/−) mice. J Bone Miner Res 2008; 23: 1815–1824. [PubMed: 18597625] * Cited only in supplementary material.

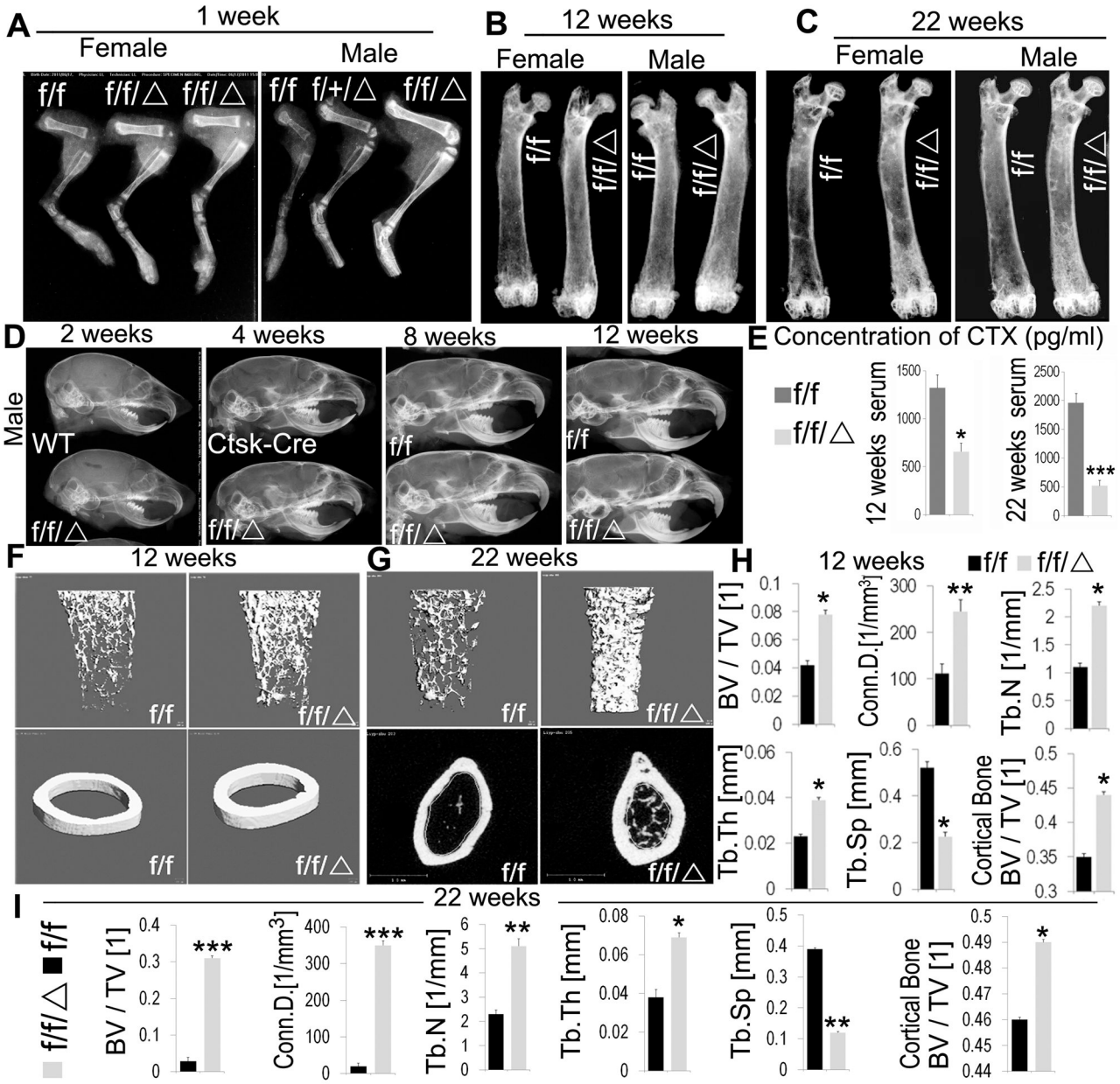

Figure 1. Mice with *Ctsk-Cre* mediated conditional knockout of C/ebpα develop severe osteopetrosis in a temporal manner.

(**A-C)** Radiographic analysis of male and female mouse femurs at various skeletal development time points: 1 (N=17), 12 (N=20), and 22 wk (N=19). (**D)** Radiographic analysis of male and female mouse cranial development to assess tooth eruption and skull phenotype. (**E)** Bone resorption assay measuring mouse serum carboxy-terminal collagen crosslinks (CTX) concentration in 12-wk-old and 22-wk-old mice, N=30 including male and female mice. **(F, G)** μCT of femurs from 12-wk-old and 22-wk-old female mice; N=12. **(H, I)** Bone density analysis of F and G, respectively. Labels: (BV) bone volume, (TV) total bone volume. (Conn.D) connectivity density, (Tb.N) trabecular number, (Tb.Sp) trabecular

separation, (Tb.Th) trabecular thickness. Results are presented as mean ± SD of triplicate independent samples. *p<0.05, **p<0.01, ***p<0.005. NS, not significant.

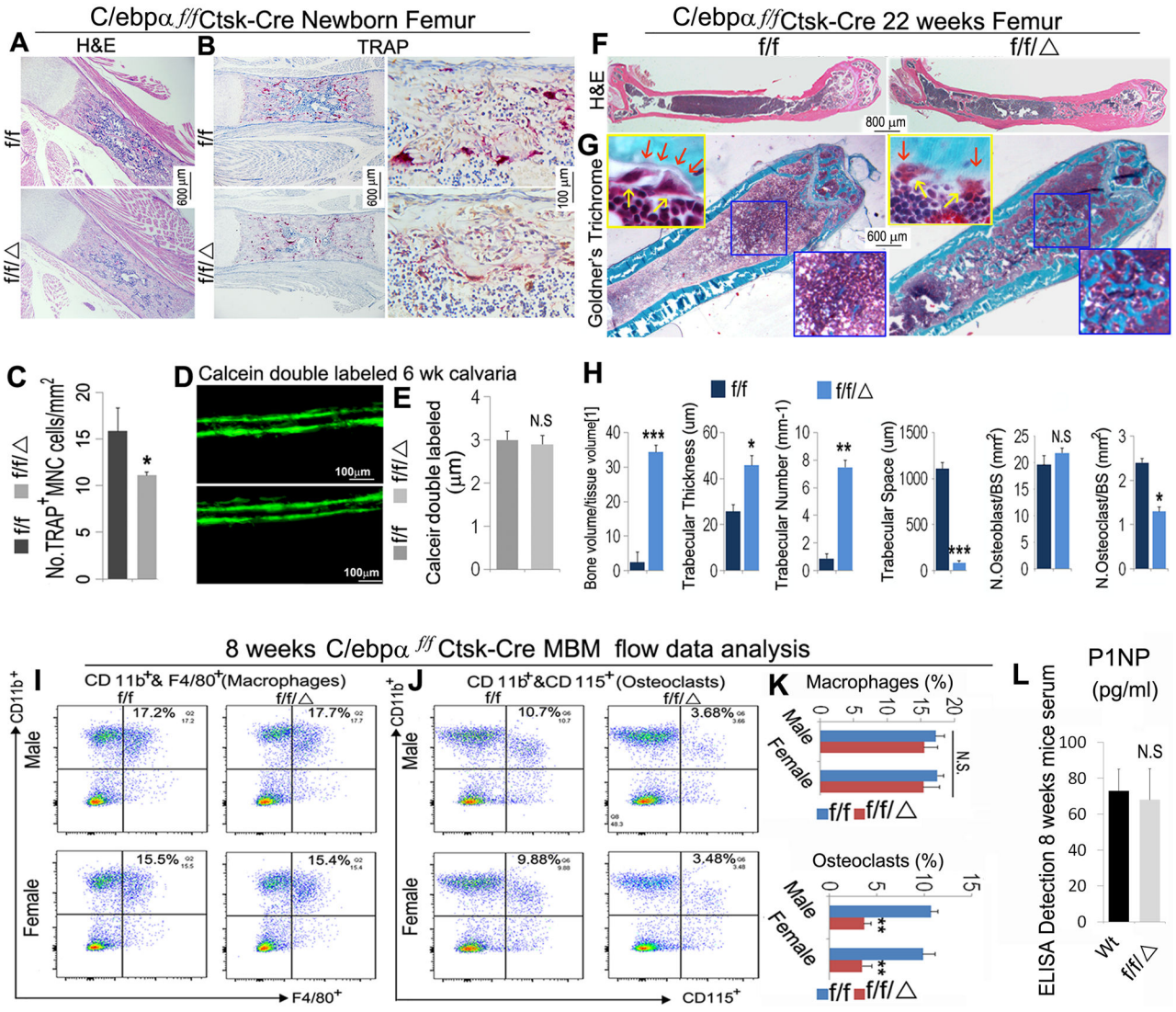

Figure 2. *C/ebpα*$^{f/f}$*Ctsk-Cre* mice show significantly impaired osteoclast polarization and function, with no changes in bone formation or macrophage development.

(A) H&E staining and **(B)** TRAP staining (osteoclast-like marker) of newborn *C/ebpα*$^{f/f}$ *(f/f)* and *C/ebpα*$^{f/f}$*Ctsk-Cre (f/f/Δ)* mouse femurs. Higher magnification images (right column); N=20. **(C)** Quantification data for TRAP-positive cells (≥3 nuclei) in B. **(D, E)** Calcein labeling and quantification data in the calvariae assessed using non-decalcified frozen sections showed no significant changes in calvarial bone formation after CKO of *C/ebpα*; N=20. **(F)** H&E stain of 22-wk-old male and female mouse femurs, followed by **(G, H)** Goldner's Trichrome analysis suggested that the degree of osteopetrosis due to *C/ebpα* CKO has become more severe in older mice with no change in osteoblast number; N=4. **(I, J)** Flow cytometry for **(I)** immune cell subtyping of CD11b+ F4/80+ macrophages and **(J)** CD11b+CD115+ osteoclasts of 8-wk-old mouse none marrow (MBM). **(K)** Quantification of I and J. **(L)** ELISA detection of P1NP (pg/mL) in 8-wk-old mouse serum indicating bone formation is not affected by gene CKO. Bars show means ± SD. of triplicate independent samples. *p<0.05, **p<0.01, ***p<0.005. NS, not significant.

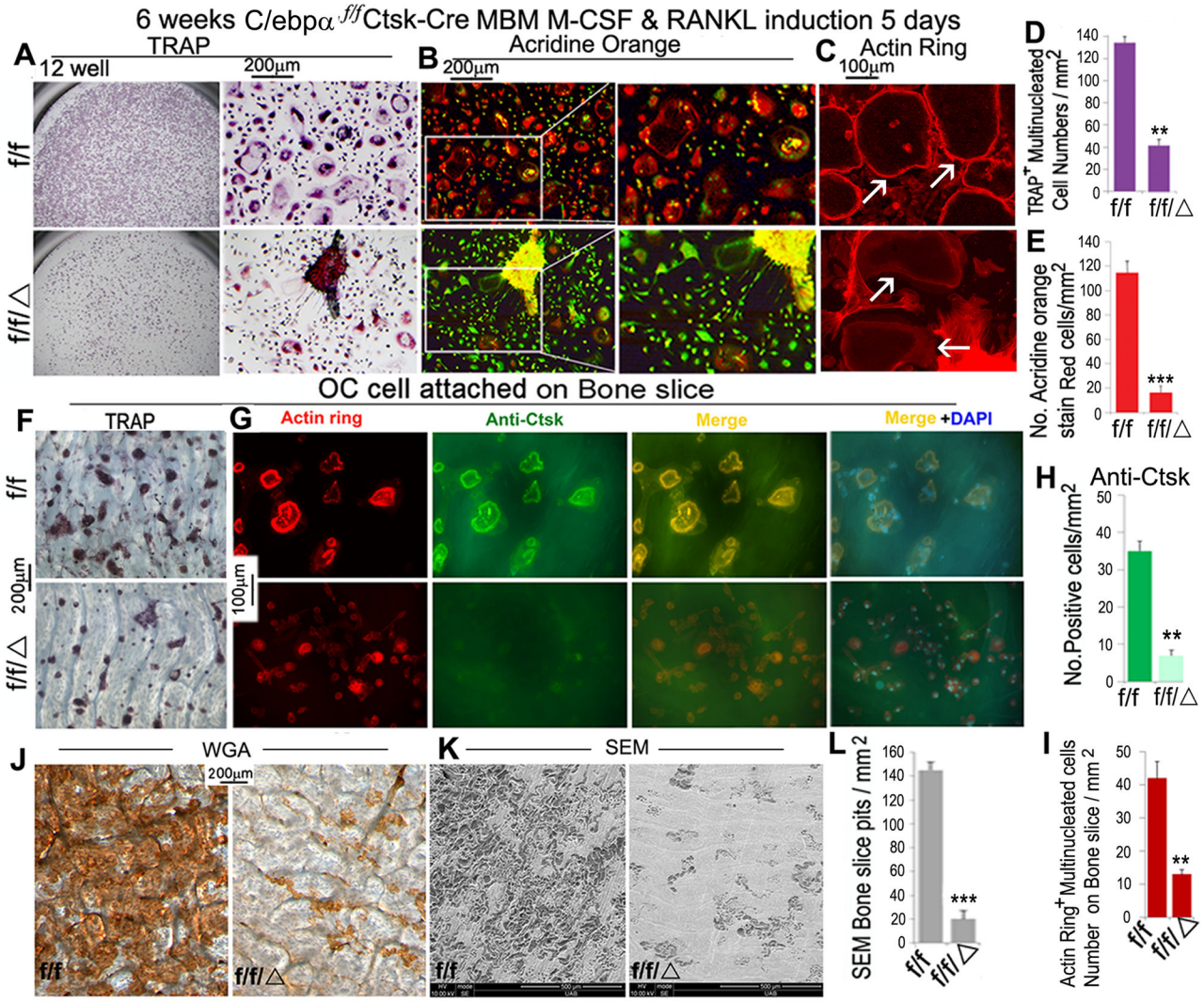

Figure 3. Conditional knockout of C/ebpα results in severely defective osteoclast activation and function, leading to diminishing osteoclastic bone resorption *in vitro*.

(A) TRAP staining in 6-wk-old male and female *C/ebpα*$^{f/f}$*Ctsk-Cre* (f/f/Δ) mouse bone marrow (MBM) induced by M-CSF (10 ng/ml)/RANKL (10 ng/ml) compared to *C/ebpα*$^{f/f}$ (f/f) control at the end of a 5 d culture. **(B, C) (B)** acridine orange staining followed by **(C)** Actin ring formation assay showed bone resorptive activity, denoted by white arrows. **(D, E)** Quantification of **(D)** TRAP-positive MNCs (≥3 nuclei) and **(E)** acridine orange-positive cells. **(F, G)** TRAP staining, actin ring formation assay and anti-Ctsk immunostaining of osteoclasts attached on bone slices seeded with M-CSF/RANKL-induced MBM. Overlap detected as a yellow-orange area in the merged image. **(H, I)** Quantification data showed **(H)** *Ctsk* activity and **(I)** Actin ring-positive cells. **(J)** Wheat germ agglutinin (WGA) staining and **(K)** Scanning electron microcopy (SEM) analysis of osteoclasts on bone slices to detect bone resorption pits of induced MBM on bone slices. **(L)** Quantification of SEM pits on bone slices. All quantified data were expressed as the number of positive cells per mm^2 plate area (number of cells/mm^2). Results are presented as mean ± SD of triplicate independent samples; N=60. *p<0.05, **p<0.01, ***p<0.005. NS, not significant.

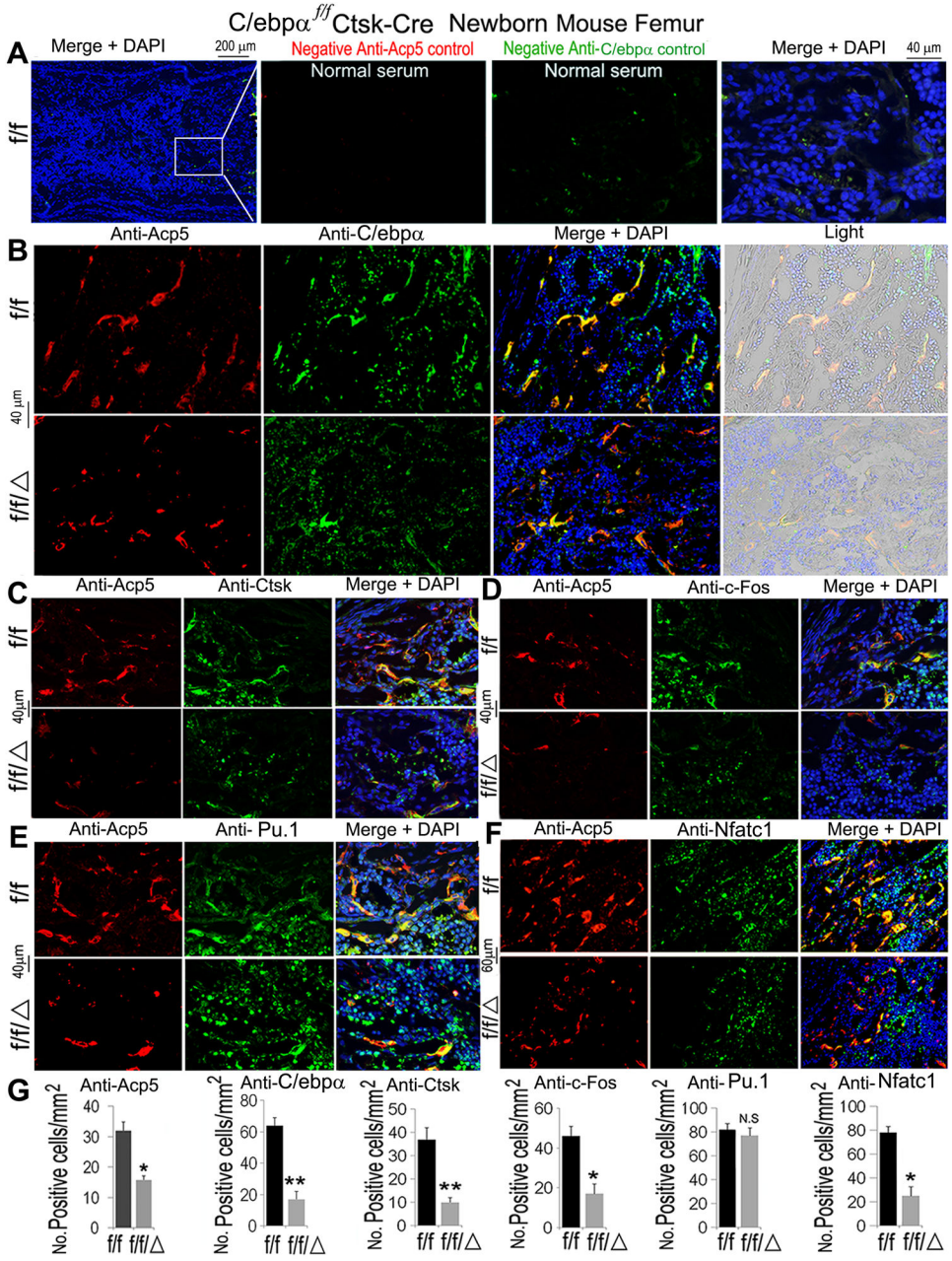

Fig 4. Conditional knockout of *C/ebpα* significantly reduces the expression of osteoclast regulators (ie. Nfatc1, c-fos) and osteoclast functional proteins (ie. Ctsk, Atp6i), but it has no effect on the expression of Pu.1 in later stage of osteoclast terminal differentiation.

(A) Immunofluorescence staining of C/ebpα (green) or Acp5 (red) in newborn femoral serial sections from *C/ebpα*$^{f/f}$ mice using normal serum as a negative control. **(B)** Immunofluorescence staining of C/ebpα (green) or Acp5 (red) in newborn femoral serial sections from *C/ebpα*$^{f/f}$*Ctsk-Cre (f/f/Δ)* and *C/ebpα*$^{f/f}$ *(f/f)* mice. **(C-F)** Immunostaining using antibodies against **(C)** Ctsk, **(D)** c-fos, **(E)** Pu.1, **(F)** Nfatc1 and their corresponding Acp5^{+} (osteoclast-like marker) merged images for newborn mouse femurs. Overlaps appears yellow-orange in the merged images. **(G)** Quantification data of B-F immunostaining

(number of positive cell/mm^2 plate area). Bars show means ± SD; N=8. *p<0.05, **p<0.01, ***p<0.005. NS, not significant.

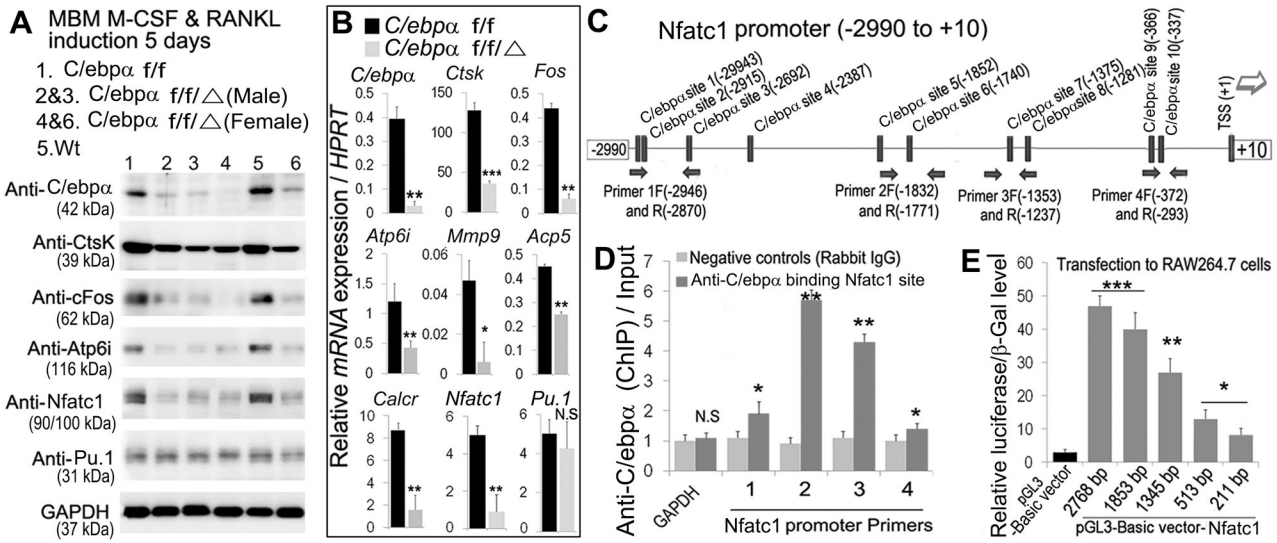

Fig 5. *C/ebpα* upregulates the expression of osteoclast regulator genes and osteoclast function genes at both protein and mRNA levels; and *C/ebpα* directly regulates Nfatc1 expression.

(A) Western blot of *C/ebpα*$^{f/f}$*Ctsk-Cre (f/f/Δ)* and *C/ebpα*$^{f/f}$ *(f/f)* M-CSF (10 ng/ml)/ RANKL (10 ng/ml)-induced MBM showing expressions of proteins important for osteoclastogenesis (*e.g.* Nfatc1, c-fos), osteoclast function (*e.g.* Ctsk, ATP6i), and a factor that is common to macrophages and osteoclasts (i.*e.* Pu.1) at the protein level. GAPDH was used as a loading control. **(B)** RT-qPCR was carried out to measure *C/ebpα*, *Ctsk*, *c-fos*, *Nfatc1*, *Atp6i*, *Mmp9*, *Acp5*, *Calcr*, and *Pu.1* mRNA levels relative to *Hprt* in M-CSF/ RANKL-induced MBM. *Hprt* served as a reference transcript. Experiments were performed nine times with independent samples (N=9). **(C)** C/ebpα directly interacts with the *Nfatc1* promoter region to induce its expression. Schematic display of *Nfatc1* (−2990/+10) promoter region: TSS (transcriptional start site), predicted C/ebpα-binding sites, and ChIP primers positions (F, Forward; R, Reverse). (**D**) ChIP analysis of C/ebpα binding to the *Nfatc1* promoter in RANKL-induced MBM using primers as indicated on the x-axis. Results are presented as ChIP/Input. **(E)** *Nfatc1* promoter fragments were inserted into the pG13-basic vector. At the end of 2-day culture to promote osteoclast formation, RANKL-induced RAW264.7 cells were transfected with pG13-*C/ebpα*−2768bp,−1853bp,−1345bp,−513bp, −211bp. Luciferase was detected at 48 h post-transfection and normalized to β-gal activity. Bars show means ± SD. *p<0.05, **p<0.01, ***p<0.005. NS, not significant.

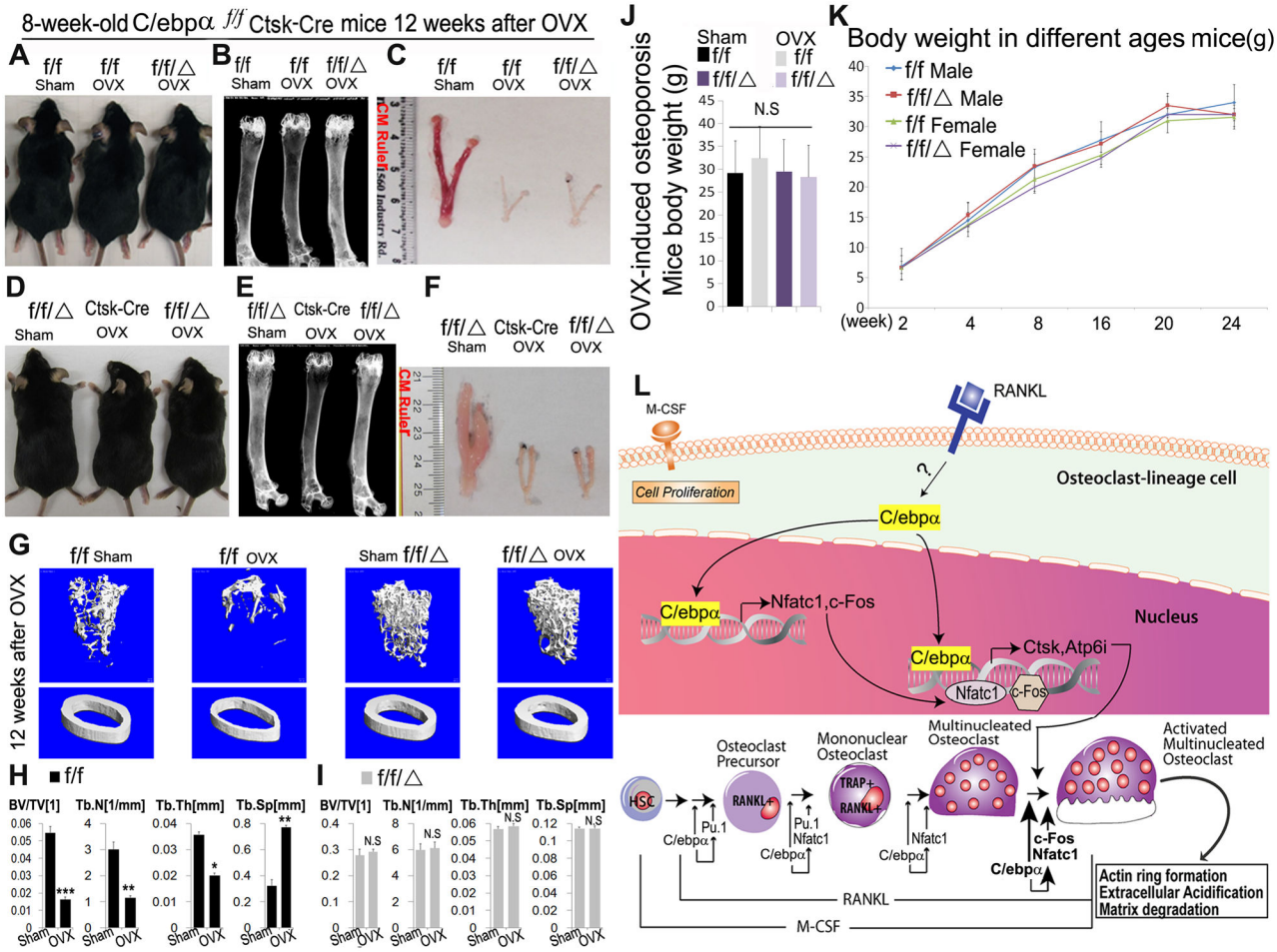

Fig 6. The deficiency of C/ebpα in osteoclasts blocks ovariectomy (OVX)-induced bone loss in osteoporosis mouse model and proposed working model for the mechanism underlying C/ebpα's roles in osteoclast terminal differentiation.

C/ebpα's roles in OVX-induced bone loss analysis were examined in 8-week-old *C/ebpα*$^{f/f}$ (f/f), *Ctsk-Cre* and *C/ebpα*$^{f/f}$*Ctsk-Cre* (f/f/Δ) mice at 12 weeks after sham surgery and OVX. **(A-F)** Analysis of mice includes **(A, D)** mouse photographic images, **(B, E)** radiographic analysis of mouse femurs and **(C, F)** assessment of uterine size; N=30. **(G)** μCT analysis at 12 weeks post operation. **(H, I)** Quantification data for G revealed that **(H)** OVX-*C/ebpα*$^{f/f}$ mice experienced significant bone loss compared to sham-*C/ebpα*$^{f/f}$, whereas **(I)** no significant changes were found between sham- and OVX-*C/ebpα*$^{f/f}$*Ctsk-Cre*. Bars show means ± SD. of triplicate independent samples; N=24. *p<0.05, **p<0.01, ***p<0.005. NS, not significant. **(J)** Mouse body weight assessment post OVX indicating no significant changes in normal growth between OVX and non-OVX groups; N=30. **(K)** Time-course mouse body weight assessment of male and female mice at 2, 4, 8, 16, 20, and 24 weeks showed similar body weight across male and female groups of wild-type and CKO. Results show means ± SD. *p<0.05, **p<0.01, ***p<0.005. NS, not significant. **(L)** Working model for the role of *C/ebpα* in osteoclast terminal differentiation. *C/ebpα,* which is induced by RANKL, is important for the expression of important osteoclast regulator and function

genes, which regulate osteoclast terminal differentiation leading to cell activation and function.